

Large Area 2D and 3D Colloidal Photonic Crystals Fabricated by a Roll-to-Roll Langmuir–Blodgett Method

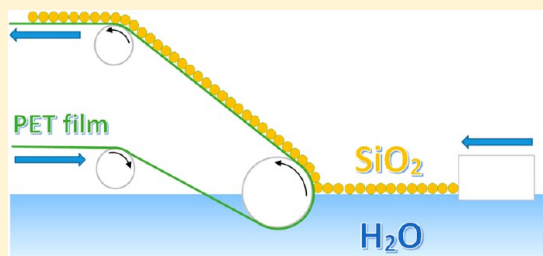
Mikhail Parchine,^{*,†} Joe McGrath,[†] Maria Bardosova,^{†,‡} and Martyn E. Pemble^{†,§}

[†]Tyndall National Institute, UCC, Lee Maltings, Dyke Parade, Cork, Ireland

[‡]Institute of Electronics and Photonics, Faculty of Electrical Engineering and Information Technology, Slovak Technical University, Bratislava, Slovakia

[§]Department of Chemistry, University College Cork, Cork, Ireland

ABSTRACT: We present our results on the fabrication of large area colloidal photonic crystals on flexible poly(ethylene terephthalate) (PET) film using a roll-to-roll Langmuir–Blodgett technique. Two-dimensional (2D) and three-dimensional (3D) colloidal photonic crystals from silica nanospheres (250 and 550 nm diameter) with a total area of up to 340 cm² have been fabricated in a continuous manner compatible with high volume manufacturing. In addition, the antireflective properties and structural integrity of the films have been enhanced via the use of a second roll-to-roll process, employing a slot-die coating of an optical adhesive over the photonic crystal films. Scanning electron microscopy images, atomic force microscopy images, and UV–vis optical transmission and reflection spectra of the fabricated photonic crystals are analyzed. This analysis confirms the high quality of the 2D and 3D photonic crystals fabricated by the roll-to-roll LB technique. Potential device applications of the large area 2D and 3D colloidal photonic crystals on flexible PET film are briefly reviewed.



INTRODUCTION

One of the intriguing properties of photonic crystals is that they possess a photonic bandgap which does not allow the propagation of light with certain wavelengths in certain directions. The origin of the photonic bandgap is the periodic variation of refractive index in photonic crystals. Many objects in nature have photonic crystal structures that allow manipulation of light and create bright colors. For example, peacock feathers have two-dimensional photonic crystal structures and natural opals have three-dimensional photonic crystal structures.

Since the pioneering theoretical work of Yablonovitch and John,^{1–3} many useful applications of photonic crystal structures have been developed in optoelectronics, photovoltaics,⁴ sensors,^{5,6} and energy storage.⁷ However, it may be argued that the assembly of colloidal particles—the simplest and cheapest means of fabricating photonic crystals in a manner that mimics the structures found in natural opals—has not found commercial application due to two fundamental limitations, namely the lack of control over the fabrication process and the lack of scalability toward high volume manufacturing.

Colloidal photonic crystals (or artificial opals) can be easily fabricated via self-assembly of colloidal monodisperse spheres of dielectric materials. Different fabrication methods can be used: controlled evaporation,^{8,9} spin coating,¹⁰ and Langmuir–Blodgett.¹¹ Among these methods, the Langmuir–Blodgett (LB) method is one of the fastest, versatile, and scalable techniques that allows fabrication of two-dimensional (2D) and

three-dimensional (3D) photonic crystal structures with full control over the amount of layers deposited and the composition of each layer, thus addressing the first limitation noted above. However, many possible applications of the LB method (and also the other fabrication methods) are limited by the size of the substrate for deposition of photonic crystal structures. For large area applications, such as thin film solar photovoltaic panels, flexible polymer solar cells, flexible OLEDs, colloidal lithography, and others, a roll-to-roll LB method must be developed for the deposition of photonic structures on a flexible substrate, for example, poly(ethylene terephthalate) (PET) film, and in so doing address the second limitation noted above.

In this paper, we report the fabrication of the large area colloidal photonic crystals using a roll-to-roll LB technique. Colloidal silica spheres with two diameters were used: $D_1 = 250$ nm and $D_2 = 550$ nm. High quality 2D hexagonal arrays of silica spheres with a total area up to 340 cm² were deposited on a flexible PET substrate. We demonstrate that also 3D large area photonic crystals can be fabricated by our roll-to-roll LB method. High-resolution scanning electron microscopy images, atomic force microscopy images, and optical transmission and reflection spectra of the fabricated samples are analyzed. Some potential practical applications of the large area colloidal photonic crystals are also discussed.

Received: April 1, 2016

Revised: May 23, 2016

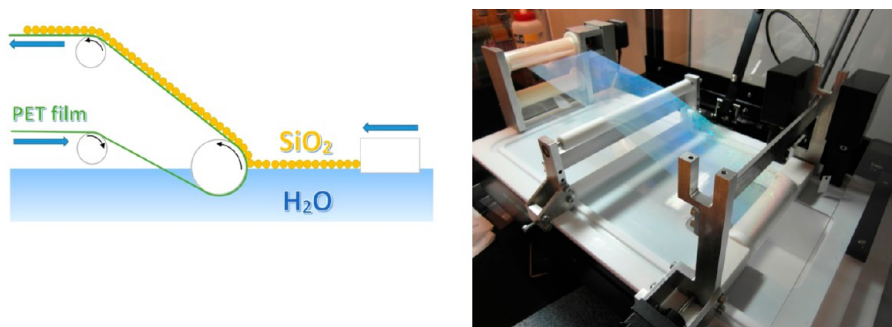


Figure 1. Left: schematic representation of the roll-to-roll LB method. Right: photograph of the NIMA trough, the roll-to-roll unit, and the PET substrate with a LB monolayer of silica spheres deposited ($D_2 = 550$ nm).

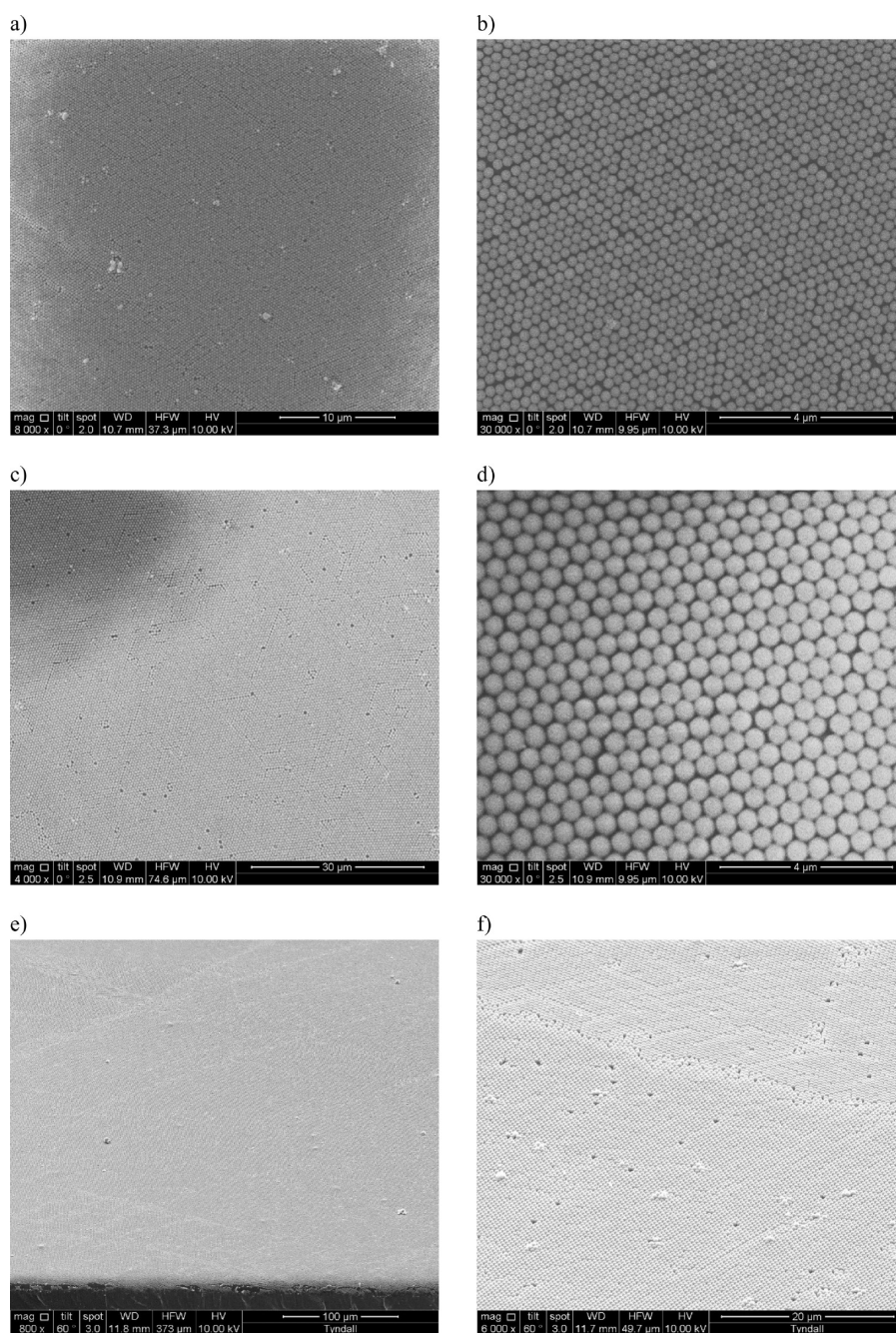


Figure 2. SEM images of the monolayer of silica spheres $D_1 = 250$ nm (a, b) and $D_2 = 550$ nm (c–f) deposited on the PET film using the roll-to-roll LB method. The parameters used for the LB process are described in the [Experimental Section](#).

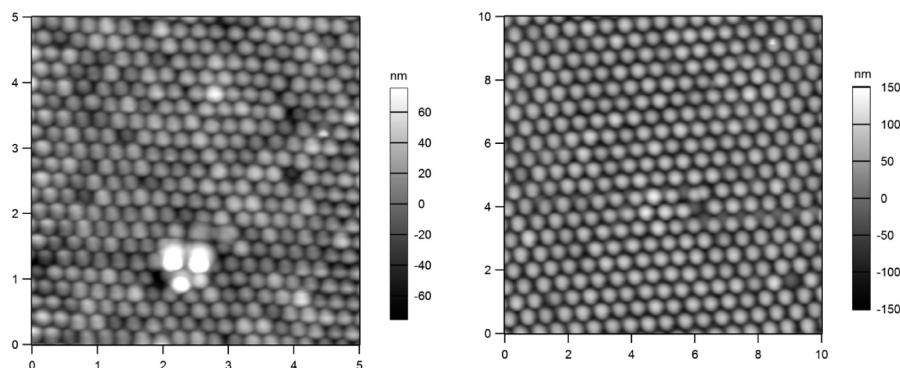


Figure 3. AFM images of the monolayer of silica spheres $D_1 = 250$ nm (left) and $D_2 = 550$ nm (right) deposited on the PET film using the roll-to-roll LB method. The measured area is $5 \mu\text{m} \times 5 \mu\text{m}$ for the left image and $10 \mu\text{m} \times 10 \mu\text{m}$ for the right one.

EXPERIMENTAL SECTION

Poly(ethylene terephthalate) (PET) film was purchased from HiFi Industrial Film. This film is highly transparent film and has a thickness of $50 \mu\text{m}$. In order to obtain the hydrophilic surface, required for high quality Langmuir–Blodgett deposition of silica spheres, the PET film was pretreated in an oxygen plasma for 3 min, using a Harrick Plasma Cleaner (PDC-002) with maximum power of 200 W and a working pressure of 150–200 mTorr. Contact angle measurements were performed before and after the treatment to check the hydrophilic properties of the film surface. These measurements have shown good hydrophilic properties with the average contact angle value decreasing from 78° before treatment to 11° after treatment.

Colloidal monodispersed silica spheres with diameters 250 nm ($\pm 4.4\%$) and 550 nm ($\pm 2.8\%$) were synthesized using a modified Stöber method¹² involving the hydrolysis of tetraethyl orthosilicate (TEOS) in the presence of ethanol and ammonium hydroxide as a catalyst. Each preparation was performed at room temperature under constant magnetic stirring for 24 h, followed by removal of unreacted TEOS and ammonia by repeated centrifuging, washing–sonication cycles in ultrapure water and ethanol. Tetraethyl orthosilicate (TEOS), ammonium hydroxide (25%), and ethanol (100%) were purchased from Sigma-Aldrich and used as received without further purification. Ethanol was filtered through Whatmann filter papers before use to remove any particulate impurities. Ultrapure water ($18.2 \text{ M}\Omega\text{-cm}$) was used directly from a Millipore water system.

For the Langmuir–Blodgett deposition process of silica spheres on the PET film we use a NIMA trough (model 1222D2). The standard alternate dipper mechanism in the NIMA trough was replaced by a special roll-to-roll unit (Figure 1). The roll-to-roll unit was developed in the framework of the EU FP7 project ALBATROSS (grant agreement 324449) by Microtestmachines (Belarus).¹³ Initially, a suspension of silica spheres in ethanol with a concentration of 0.03 g/mL was diluted with chloroform in a ratio of 1:4, respectively. Then, a small quantity of the solution was spread on the air/water interface. For all experiments double distilled deionized water with a resistivity $18.2 \text{ M}\Omega\text{-cm}$ was used as the subphase. Silica particles with a diameter 550 nm were made hydrophobic using the surfactant 3-(trimethoxysilyl)propyl methacrylate (TPM), and silica particles with a diameter 250 nm were used without adding any surfactant. Previous investigations^{11,14} have revealed that this procedure is necessary for silica spheres with a diameter above 400 nm since it facilitates the floating of the particles at the air/water interface and leads to formation of a stable film. However, for smaller silica spheres (180–360 nm) good quality LB films can be made without the addition of surfactants. After spreading, the film was compressed using the barrier with a speed $12 \text{ cm}^2/\text{min}$ to a surface pressure of 5 mN/m, which was stabilized during the whole LB deposition process. The surface pressure–trough area (P – A) isotherms were used for the LB deposition monitoring. From the isotherms a deposition ratio was determined. The deposition ratio is equal to $\Delta A/A_{\text{PET}}$, where ΔA is

the change of the trough area during deposition and A_{PET} is the area of the PET film used for the deposition process.

During the roll-to-roll LB deposition process the PET film was moved by a stepping motor around a rotating barrier in the center of the trough (the deposition zone) with a constant velocity of 3 mm/min. The rotating barrier separates the NIMA trough in two compartments: A and B. Compartment A contains pure water and compartment B the monolayer of silica particles stabilized on the air/water interface. The PET film rotates through the air/water interface in compartment A and rises up through the air/water interface in compartment B. The LB layer is deposited by raising the PET film from the water through the monolayer of silica spheres (Figure 1). The total area of the LB trough (part B) is equal to 520 cm^2 . After spreading silica nanospheres on the air/water interface followed by compression to the dense monolayer, the total area of the dense film was equal to 400 – 420 cm^2 . The deposition ratio during the process was equal to 100%. Since the stop position of the barrier is 70 cm^2 , a dense monolayer of silica nanospheres with a total area of up to 350 cm^2 can be deposited on the PET film.

A high-resolution scanning electron microscope (HRSEM, Quanta FEG 650, FEI Company) was used to characterize the fabricated samples with 2D and 3D photonic crystal structures. During SEM investigations, samples were gold-sputtered prior to examination to avoid charging effects. An atomic force microscope (MFP-3D, Asylum Research) was used for topographic imaging of the fabricated colloidal photonic crystal films.

Optical characterization was performed using a Mikropack halogen HL2000 white light source, with a focused spot size at the sample of approximately 1.5 mm diameter. The transmitted or reflected light was collected via an optical fiber to an Ocean Optics HR4000 detector for wavelengths in the UV–vis range. Spectral analysis was performed using Ocean Optics software SpectraSuite. Reflectance measurements were calibrated against a Thor Laboratories ME1-PO1 silver mirror. Transmission calibration was made with respect to air. Transmission spectra of the samples were acquired at the angle of incidence $\theta = 0^\circ$ with respect to the film normal. For reflection measurements, the angle of incidence $\theta = 10^\circ$ was used.

RESULTS AND DISCUSSION

Two samples of 2D photonic crystal structures were fabricated using the roll-to-roll LB method, using silica particles with diameters 250 and 550 nm. First, a monolayer of silica spheres $D_1 = 250$ nm was deposited on PET film with an area $10 \text{ cm} \times 32 \text{ cm}$, where 10 cm is the width of the PET film and 32 cm is the total length of the LB film. The deposition process was performed in continuous mode with the optimal parameters described in the previous section until all the available area of the trough was used. The deposition ratio calculated from the pressure–area isotherm was equal to 100%. To check the quality of the deposited monolayer, SEM images from different

areas of the PET film were analyzed. All images (Figure 2) show the high quality of the two-dimensional hexagonal structure of close-packed silica spheres.

In the second experiment, large silica spheres with $D_2 = 550$ nm were deposited using the same parameters for the roll-to-roll LB process. In this experiment the PET substrate was covered with a total LB monolayer area of 340 cm^2 . The deposition ratio was equal to 100%, indicating a reliable LB process. SEM images of different areas of the fabricated sample are shown in Figure 2. These images show the high quality 2D photonic crystal structures made from silica spheres (550 nm). However, SEM analysis of the LB monolayer on the PET film has revealed that there are large domains of silica spheres with different orientations (Figure 2f). The size of these domains varies from 1 mm^2 to around 1 cm^2 . The domains are visible to the eye due to slightly different light scattering from the ordered 2D arrays of silica spheres inside these domains. Since in the LB method a monolayer of silica spheres is transferred from the air/water interface to the substrate, these domains are most likely formed during the compression cycle of silica spheres dispersed on the air/water interface.

The surface roughness of the obtained films was analyzed by atomic force microscopy. AFM images of the two samples with 2D photonic crystal structures are presented in Figure 3. For the first sample ($D_1 = 250$ nm) the average surface roughness calculated from four different areas of $5 \mu\text{m} \times 5 \mu\text{m}$ was equal to 20 nm, with the minimum value of 13.1 nm and the maximum value of 31.2 nm. For the second sample ($D_2 = 550$ nm) the average surface roughness calculated from three different areas of $10 \mu\text{m} \times 10 \mu\text{m}$ was equal to 41 nm, with the minimum value of 27.3 nm and the maximum value of 49.1 nm.

Optical transmission spectra of two fabricated samples are shown in Figure 4. The transmission spectrum of the first

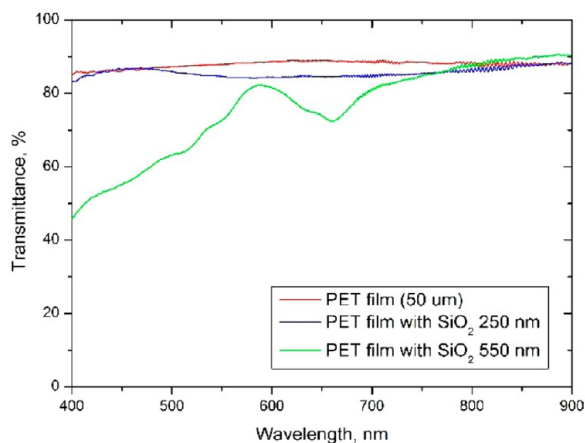


Figure 4. Transmission spectra of PET samples with LB monolayer of silica nanospheres $D_1 = 250$ nm (blue line) and $D_2 = 550$ nm (green line). For comparison, the transmission spectrum of the clean PET film is shown (red line).

sample made from small silica spheres ($D_1 = 250$ nm) shows a slight broad dip around 620 nm. Later, we demonstrate that this feature develops into a defined drop in transmission associated with a photonic bandgap as the number of LB layers increases (see Figure 10).^{15,16} The transmission spectrum of the sample with silica spheres of diameter $D_2 = 550$ nm shows a narrow minimum at 650 nm and strong attenuation below 580 nm. Earlier experimental studies have revealed that the

transmission minimum at $\lambda \sim D$ and the strong attenuation at $\lambda \leq D$ are characteristic for the 2D photonic crystal structures and are related to the excitation of surface modes and the resonant coupling of these modes with the incident light.^{17,18} The transmission minimum corresponds to the maximum in the reflection spectrum that is shown in Figure 5. This transmission minimum is due to diffraction resonance from the 2D hexagonal array of silica nanospheres and was also observed for 3D opal films.¹⁷

The optical properties of 2D arrays of silica spheres with the same diameter as those used here (550 nm) have also been studied in detail by Yamasaki and Tsutsui.¹⁸ From their optical transmission spectra at different angles and polarizations of incident light, they obtained the photonic band structure corresponding to the different crystallographic directions. They observed strong diffraction scattering of white incident light in the forward direction at different angles for different wavelengths, which is associated with the photonic band structure of the 2D photonic crystal. This scattering is very important for practical applications, for example, in thin film solar cells^{19,20} and organic light-emitting devices (OLEDs).²¹ In thin film solar cells (a-Si, flexible organic solar cells) this diffraction of the incident light will increase an effective optical absorption in very thin photoactive layers, resulting in higher photocurrent and total power conversion efficiency (up to 10–15%). Such light trapping photonic structures will be beneficial for photovoltaic panels, especially, for countries with lower light conditions. An additional advantage of the 2D photonic crystal layer is that the enhancement of optical absorption is almost insensitive to the incident angle of the sunlight.¹⁹ This therefore could be used in building-integrated photovoltaics, for example, on vertical surfaces where reflection of the sunlight is not desirable. In OLEDs, the application of 2D photonic crystals will significantly enhance the light out-coupling factor and the total electroluminescent efficiency. This was demonstrated by Yamasaki et al.²¹ for OLEDs with integrated monolayers of the ordered array of silica spheres again with $D = 550$ nm.

For practical applications, for example, in thin film solar cells and flexible OLEDs, the 2D photonic crystal made from silica nanospheres must be permanently fixed to the PET film surface and must be robust. For this purpose an optical adhesive was used, NOA164 (Norland Optical Adhesive 164), which has the relatively high refractive index of 1.64. A thin layer (5 μm) of the NOA164 was coated above the monolayer of silica spheres with diameter $D_2 = 550$ nm by using a roll-to-roll slot-die coater (Figure 5), employed so as to specifically demonstrate the utility of combining two roll-to-roll processing methods so as to produce the final working structure.

Optical transmission spectra of the coated and uncoated samples are shown in Figure 6. One can see that in the spectral region above 500 nm the coated sample exhibits higher transmittance than that of the original uncoated sample and also of the clean PET film. The transmission minimum at 650 nm has disappeared after coating with NOA164. The antireflective properties of the coated sample are also confirmed by the reflection spectra (Figure 5). Reflectance of the coated sample in the visible and near-infrared spectrum range is 3–4% lower than that of the clean PET film. This is due to the high transparency of the optical adhesive in this spectral region: optical transmission through 25 μm film thickness increases from 96.1% at 450 nm to 99% at 1500 nm, according to Norland specifications. It is important that the strong light

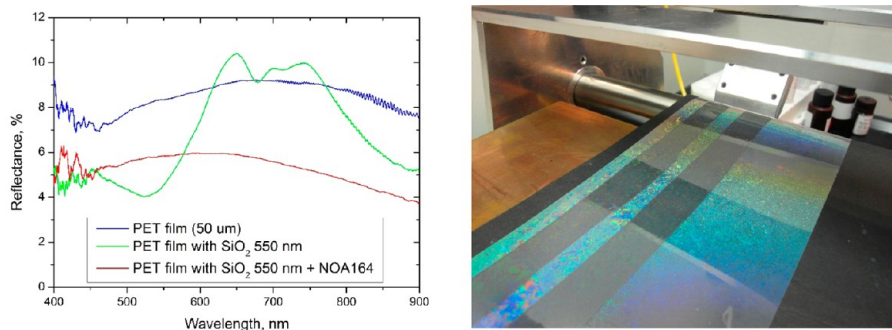


Figure 5. Left: reflection spectra of the clean PET film (blue line), PET sample with LB monolayer of silica nanospheres $D_2 = 550$ nm (green line), and PET sample with LB monolayer of silica nanospheres $D_2 = 550$ nm coated with optical adhesive NOA164 (red line). Right: photograph of the roll-to-roll slot-die coating with strips of optical adhesive NOA164 on the PET substrate with the LB monolayer of silica spheres $D_2 = 550$ nm.

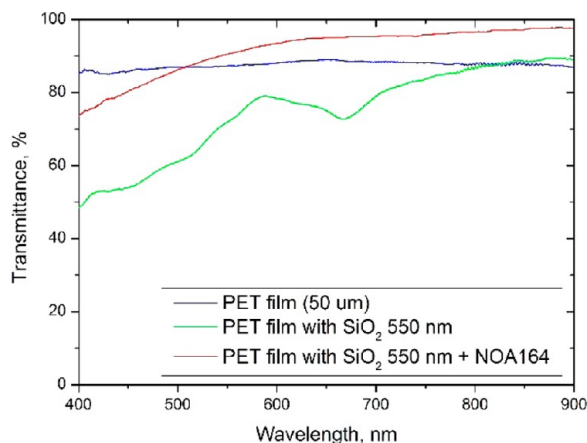


Figure 6. Transmission spectra of the second PET sample with LB monolayer of silica nanospheres $D_2 = 550$ nm (green line) and the same sample coated with optical adhesive NOA164 (red line). For comparison, transmission spectrum of the clean PET film is shown (blue line).

scattering properties observed in the uncoated sample at $\lambda \leq D$ are preserved after coating with NOA164 (Figure 6). Thus, we conclude that roll-to-roll coating with an optical adhesive that has a high refractive index can be used as part of the fabrication and potential large-scale integration of large area 2D photonic crystals made from silica spheres by the roll-to-roll LB method in practical devices.

It is also noteworthy that large area 2D colloidal crystals fabricated by the roll-to-roll LB method can be used in large scale colloidal nanolithography.²² The 2D structures of nanospheres can be transferred by a simple offset printing

method from the PET film to different substrates. An important issue for colloidal lithography is the long-range order in the 2D close-packed arrays of nanospheres. To improve the quality of fabricated LB films, monitoring by Brewster angle microscopy (BAM) can be used during the roll-to-roll LB process.^{23,24} We suggest that BAM monitoring will be very helpful in establishing the optimal deposition parameters required in order to achieve the most stable and uniform monolayers at the air/water interface: for instance, to establish the best conditions of surface pressure, compression speed, and addition of surfactants for nanoparticles functionalization. The quality of the nanospheres used is also crucial in order to obtain long-range order in 2D colloidal crystals. Recently, crystallographic defects found in 2D colloidal photonic crystals made from polystyrene and silica microspheres have been analyzed qualitatively and quantitatively by using SEM, using Fourier transforms taken from the SEM images together with optical measurements.²⁵ From this analysis, two main limiting factors for the fabrication single domain 2D colloidal crystals have been determined, namely, the presence of spheres smaller than the average diameter and nonspherical particle formation (doublets or nonspherical structures). It has been suggested that in order to minimize the formation of defects such as dislocations and rotated domains, the polydispersity must be below 3% and the amount of different sized and shaped particles must also be very low.²⁵

In terms of emerging applications of these materials, recent progress has been achieved in the fabrication of novel biochemical colorimetric sensors as reported by Cai et al.⁶ Such sensors may benefit directly from the development of the roll-to-roll technologies described here. In their work, Cai et al. utilized the strong diffraction of light in the forward direction

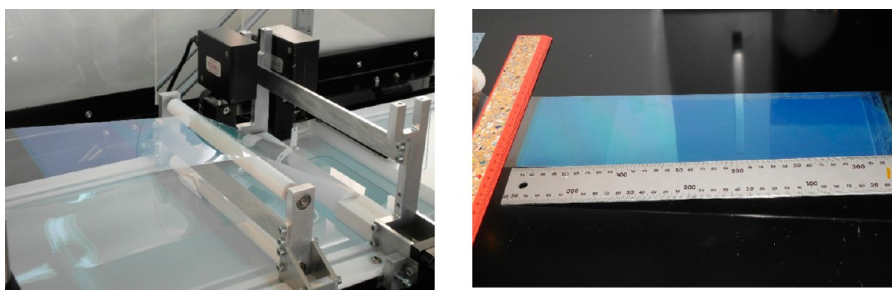


Figure 7. Photographs of the 3D colloidal photonic crystals made from silica spheres $D_1 = 250$ nm. Four and five LB layers were deposited on the PET film using the roll-to-roll LB method. The first part (from the left) of the sample has four LB layers covering an area of $8 \text{ cm} \times 10 \text{ cm}$, and the second part of the sample has five LB layers covering $24 \text{ cm} \times 10 \text{ cm}$.

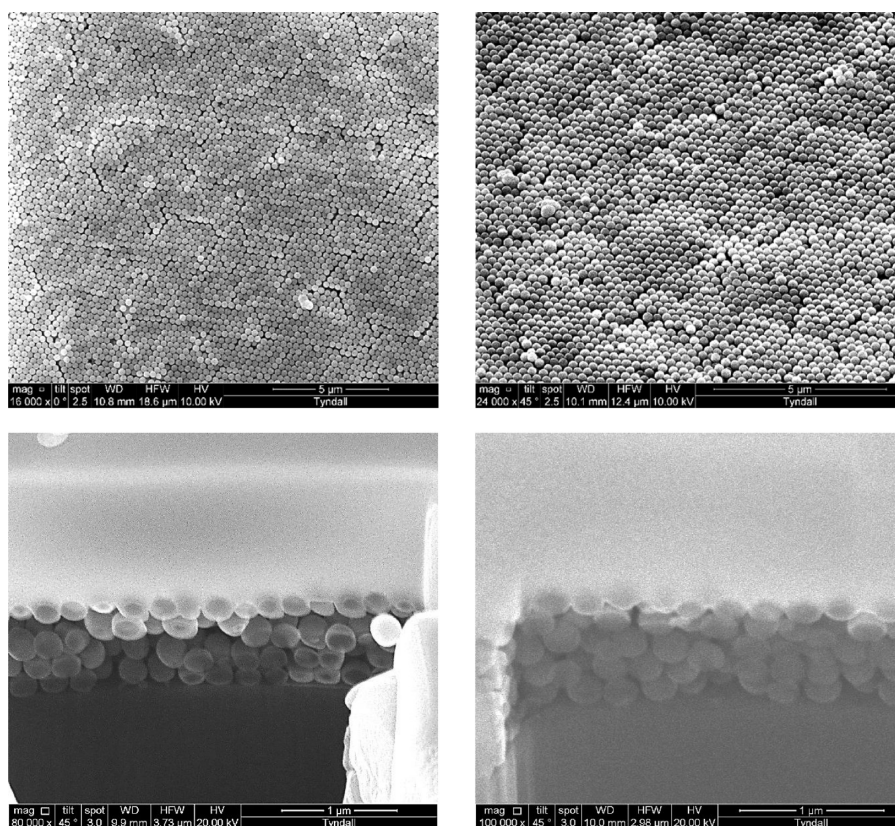


Figure 8. SEM images of the 3D colloidal photonic crystal made from silica spheres $D_1 = 250$ nm. First row: surface images of the sample with five LB layers deposited on the PET film using the roll-to-roll method. Second row: cross-sectional SEM images of the two samples—sample with 4 layers (left) and sample with 5 layers (right).

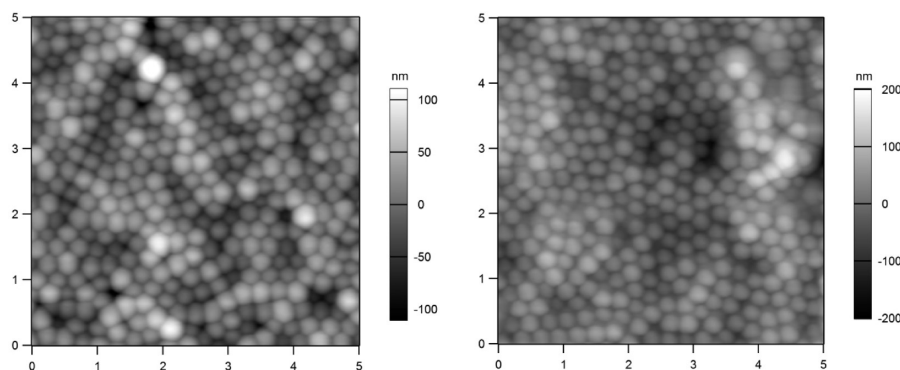


Figure 9. AFM images of the 3D colloidal photonic crystal made from silica nanospheres $D_1 = 250$ nm by the roll-to-roll LB technique (sample with five layers). Two different regions with $5 \mu\text{m} \times 5 \mu\text{m}$ are shown.

by the 2D hexagonal arrays in their sensing devices. The 2D colloidal photonic crystals were embedded into the surfaces of polymer hydrogels, which are responsive to different chemical species. Volume phase transitions, which take place in such hydrogels as a response to analytes, swell or shrink the hydrogels and therefore change the spacing in 2D photonic crystals and shift their diffraction wavelengths. These color changes can then be visually detected. We propose that our large area 2D photonic crystals fabricated using the roll-to-roll technologies described could be easily integrated into manufacturing processes of colorimetric sensors: indeed, the polymer hydrogels could be coated onto the 2D photonic crystals by using roll-to-roll coating equipment such as the slot-

die or wire coaters. Experiments of this nature are currently underway in our laboratories.

An important issue for large scale applications of the roll-to-roll LB technologies for assembling colloidal photonic crystal structures is the use of eco-friendly spreading solvents replacing chloroform. Recently, an electrospray-assisted spreading method has been reported, which enables LB deposition of colloidal particles dissolved in water and alcohol-based solvents.²⁶ For example, this method was successfully employed for spreading and LB assembly of polystyrene (PS) nanospheres from a 1:1 ethanol–water solution.

In the last experiments described here, a sample with a large area 3D photonic crystal structure was fabricated by this roll-to-roll LB method, using silica particles with diameter $D_1 = 250$

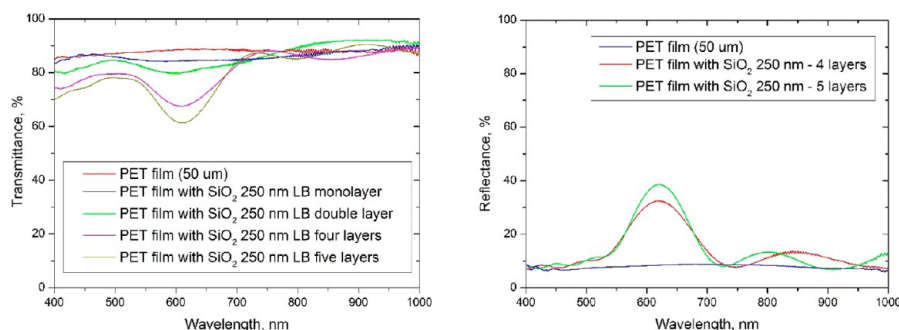


Figure 10. Left: transmission spectra of the PET samples with 2D and 3D colloidal photonic crystals made from silica nanospheres $D_1 = 250$ nm by the roll-to-roll LB technique. Right: reflection spectra of the 3D colloidal photonic crystals made from silica nanospheres $D_1 = 250$ nm by roll-to-roll LB technique: the PET sample with four LB layers of silica nanospheres (red line), the PET sample with five LB layers of silica nanospheres (green line), and the clean PET film (blue line).

nm (Figure 7). The fabrication process includes repeating the LB deposition of a colloidal film monolayer as explained in the Experimental Section. The first part of the sample has four LB layers covering an area of $8 \text{ cm} \times 10 \text{ cm}$, after which five LB layers were produced covering an area of $24 \text{ cm} \times 10 \text{ cm}$. SEM images of the surface from different areas of the sample with five LB layers and also cross-sectional SEM images of the two samples (4 and 5 layers) are shown in Figure 8. These images show the high quality of the 3D photonic crystal structures. For creating the cross sections SEM Quanta 3D 200i (FEI Company) was used. Before cutting the cross section using an ion beam a thin layer ($0.8 \mu\text{m}$) of platinum was deposited on the surface ($10 \mu\text{m} \times 10 \mu\text{m}$) of the photonic crystal film using a gas injection system.

The surface roughness of the 3D photonic crystal film was analyzed using AFM measurements. AFM images of the sample with five LB layers are presented in Figure 9. The average value of surface roughness calculated from three different areas of $5 \mu\text{m} \times 5 \mu\text{m}$ is equal to 42.5 nm , with the minimum value of 28.2 nm and the maximum value of 53.6 nm . We see that the surface roughness for the sample with five LB layers has increased by a factor of 2 in comparison with the value for the sample with a single LB layer ($D_1 = 250 \text{ nm}$).

Contact angle measurements were performed to check the hydrophilic properties of the fabricated 2D and 3D photonic crystal films. These measurements have shown good hydrophilic properties with the average contact angle values of 21° – 23° , which are not dependent on the number of layers (for small nanospheres $D_1 = 250$) or the size of silica spheres (250 and 550 nm).

Optical transmission and reflection spectra of the fabricated 3D photonic crystals are shown in Figure 10. The first Bragg reflection peak at 620 nm is observed, which corresponds to the minimum in the transmission spectra. The optical transmission spectra from different areas of the PET film were also analyzed. These spectra are almost identical indicating the high quality 3D photonic crystal structures obtained by this roll-to-roll LB technique.

Recently, Kocher-Oberlehner et al.¹⁶ have demonstrated that large area 3D colloidal photonic crystals on transparent polymer substrates can be used as planar solar concentrators for building-integrated photovoltaics. In this work colloidal photonic crystals were made by a standard LB method using silica nanospheres with $D = 250 \text{ nm}$. Solar concentrators with 5 and 8 LB layers show a relative increase in total solar cell efficiency by a factor of 2 and 3, respectively. Large area 3D

photonic crystals on flexible PET films produced by the roll-to-roll LB technique could be easily integrated into planar solar concentrators for windows and glass façades. The main advantage of such concentrators is that they use both the diffuse and direct components of sunlight, and the roll-to-roll LB method may be used to reduce production costs of the required modules.

CONCLUSIONS

We have demonstrated that high quality large area 2D and 3D colloidal photonic crystals can be fabricated on a flexible PET film by a roll-to-roll LB method. Monodispersed colloidal silica nanospheres with diameters of 250 and 550 nm were used to prepare 2D photonic crystals with a total area of 340 cm^2 . Also by this method large area 3D photonic crystals were produced using silica nanospheres (250 nm). For the LB deposition process a standard NIMA trough equipped with a special roll-to-roll unit was used. SEM, AFM, optical transmission, and reflection characterization confirm the high quality of these 2D and 3D photonic crystals. The LB method is well-known for the production of monolayers and has been shown to be scalable for the production of large scale 2D and 3D colloidal photonic crystal structures on flexible substrates. We have also demonstrated that the antireflection properties and the structural robustness of the films can be significantly enhanced via a coating of optical adhesive also applied via a roll-to-roll technique.

We believe that our work will stimulate industrial device applications of photonic crystals for solar photovoltaics, nanoelectronics, and chemical and biochemical sensors.

AUTHOR INFORMATION

Corresponding Author

*(M.P.) E-mail mikhail.parchine@tyndall.ie.

Notes

The authors declare no competing financial interest.

ACKNOWLEDGMENTS

The authors gratefully acknowledge financial support from EU FP7 via ALBATROSS project, Grant Agreement 324449, and Science Foundation Ireland Principal Investigator Grant SFI 11/PI/1117. The authors thank Dr. Lynette Keeney and Vince Lodge (Tyndall National Institute) for their help with the AFM and cross-sectional SEM measurements.

REFERENCES

- (1) Yablonovitch, E. Inhibited Spontaneous Emission in Solid-State Physics and Electronics. *Phys. Rev. Lett.* **1987**, *58*, 2059–2062.
- (2) John, S. Strong Localization of Photons in Certain Disordered Dielectric Superlattices. *Phys. Rev. Lett.* **1987**, *58*, 2486–2489.
- (3) Yablonovitch, E.; Gmitter, T. J. Photonic Band Structure: The Face-Centered-Cubic Case. *Phys. Rev. Lett.* **1989**, *63*, 1950–1953.
- (4) Karg, M.; König, T. A. F.; Retsch, M.; Stelling, C.; Reichstein, P. M.; Honold, T.; Thelakkat, M.; Fery, A. Colloidal self-assembly concepts for light management in photovoltaics. *Mater. Today* **2015**, *18*, 185–205.
- (5) Wang, H.; Zhang, K. Photonic Crystal Structures with Tunable Structure Color as Colorimetric Sensors. *Sensors* **2013**, *13*, 4192–4213.
- (6) Cai, Z.; Smith, N. L.; Zhang, J. T.; Asher, S. A. Two-Dimensional Photonic Crystal Chemical and Biomolecular Sensors. *Anal. Chem.* **2015**, *87*, 5013–5025.
- (7) Armstrong, E.; O'Dwyer, C. Artificial opal photonic crystals and inverse opal structures – fundamentals and applications from optics to energy storage. *J. Mater. Chem. C* **2015**, *3*, 6109–6143.
- (8) Jiang, P.; Bertone, J. F.; Hwang, K. S.; Colvin, V. L. Single-Crystal Colloidal Multilayers of Controlled Thickness. *Chem. Mater.* **1999**, *11*, 2132–2140.
- (9) Norris, D. J.; Arlinghaus, E. G.; Meng, L.; Heiny, R.; Scriven, L. E. Opaline Photonic Crystals: How Does Self-Assembly Work. *Adv. Mater.* **2004**, *16*, 1393–1399.
- (10) Fang, Y.; Phillips, B. M.; Askar, K.; Choi, B.; Jiang, P.; Jiang, B. Scalable bottom-up fabrication of colloidal photonic crystals and periodic plasmonic nanostructures. *J. Mater. Chem. C* **2013**, *1*, 6031–6047.
- (11) Bardosova, M.; Pemble, M. E.; Povey, I. M.; Tredgold, R. H. The Langmuir-Blodgett Approach to Making Colloidal Photonic Crystals from Silica Spheres. *Adv. Mater.* **2010**, *22*, 3104–3124.
- (12) Stöber, W.; Fink, A.; Bohn, E. Controlled growth of monodisperse silica spheres in the micron size range. *J. Colloid Interface Sci.* **1968**, *26*, 62–69.
- (13) Microtestmachines ODO, Web site: <http://microtm.com/mtme.htm>.
- (14) Bardosova, M.; Dillon, F. C.; Pemble, M. E.; Povey, I. M.; Tredgold, R. H. Langmuir-Blodgett assembly of colloidal photonic crystals using silica particles prepared without the use of surfactant molecules. *J. Colloid Interface Sci.* **2009**, *333*, 816–819.
- (15) Pemble, M. E.; Bardosova, M.; Povey, I. M.; Tredgold, R. H.; Whitehead, D. Novel photonic crystal thin films using the Langmuir-Blodgett approach. *Phys. B* **2007**, *394*, 233–237.
- (16) Kocher-Oberlehner, G.; Bardosova, M.; Pemble, M.; Richards, B. S. Planar photonic solar concentrators for building-integrated photovoltaics. *Sol. Energy Mater. Sol. Cells* **2012**, *104*, 53–57.
- (17) Romanov, S. G.; Bardosova, M.; Povey, I. M.; Pemble, M. E.; Torres, C. M. S. Understanding of transmission in the range of high-order photonic bands in thin opal film. *Appl. Phys. Lett.* **2008**, *92*, 191106-1–191106-3.
- (18) Yamasaki, T.; Tsutsui, T. Fabrication and Optical Properties of Two-Dimensional Ordered Arrays of Silica Microspheres. *Jpn. J. Appl. Phys.* **1999**, *38*, S916–S921.
- (19) Grandidier, J.; Weitekamp, R. A.; Deceglie, M. G.; Callahan, D. M.; Battaglia, C.; Bukowsky, C. R.; Ballif, C.; Grubbs, R. H.; Atwater, H. A. Solar cell efficiency enhancement via light trapping in printable resonant dielectric nanosphere arrays. *Phys. Status Solidi A* **2013**, *210*, 255–260.
- (20) Yun, J.; Wang, W.; Kim, S. M.; Bae, T.-S.; Lee, S.; Kim, D.; Lee, G.-H.; Lee, H.-S.; Song, M. Light trapping in bendable organic solar cells using silica nanoparticle arrays. *Energy Environ. Sci.* **2015**, *8*, 932–940.
- (21) Yamasaki, T.; Sumioka, K.; Tsutsui, T. Organic light-emitting device with an ordered monolayer of silica microspheres as a scattering medium. *Appl. Phys. Lett.* **2000**, *76*, 1243–1247.
- (22) Zhang, J.; Li, Y.; Zhang, X.; Yang, B. Colloidal Self-Assembly Meets Nanofabrication: From Two-Dimensional Colloidal Crystals to Nanostructure Arrays. *Adv. Mater.* **2010**, *22*, 4249–4269.
- (23) Gil, A.; Guitian, F. Formation of 2D colloidal crystals by the Langmuir-Blodgett technique monitored in situ by Brewster angle microscopy. *J. Colloid Interface Sci.* **2007**, *307*, 304–307.
- (24) Gil, A.; Vaupel, M.; Guitian, F.; Möbius, D. Stress-free production and effective medium model of colloidal crystals. *J. Mater. Chem.* **2007**, *17*, 2434–2439.
- (25) Canalejas-Tejero, V.; Ibisate, M.; Golmayo, D.; Blanco, A.; López, C. Qualitative and Quantitative Analysis of Crystallographic Defects Present in 2D Colloidal Sphere Arrays. *Langmuir* **2012**, *28*, 161–167.
- (26) Nie, H.-L.; Dou, X.; Tang, Z.; Jang, H. D.; Huang, J. High-Yield Spreading of Water-Miscible Solvents on Water for Langmuir-Blodgett Assembly. *J. Am. Chem. Soc.* **2015**, *137*, 10683–10688.